

Electrochemical and spectroscopic study of the addition of several nucleophiles to 1,2,5-thiadiazole 1,1-dioxide derivatives

Silvia Lucía Aimone, José Alberto Caram, María Virginia Mirífico and Enrique Julio Vasini*

Instituto de Investigaciones Físicoquímicas Teóricas y Aplicadas (INIFTA), Facultad de Ciencias Exactas, Departamento de Química, Universidad Nacional de La Plata, Casilla de Correo 16, Sucursal 4, (1900) La Plata, Argentina

Received 3 November 1999; revised 29 December 1999; accepted 4 January 2000

ABSTRACT: The nucleophilic addition reactions of several alcohols and 1-propanethiol to a C=N double bond of 3,4-disubstituted derivatives of 1,2,5-thiadiazole 1,1-dioxide were studied in acetonitrile solution. The substrates used were 3,4-diphenyl (**1a**), 3-methyl-4-phenyl (**1b**), phenanthro[9,10-*c*] (**1c**) and acenaphtho[1,2-*c*]-1,2,5-thiadiazole 1,1-dioxide (**1d**), 3,4-diphenyl-1,2,5-thiadiazoline 1,1-dioxide (**2a**) and 4-ethoxy-5-methyl-3,4-diphenyl-1,2,5-thiadiazoline 1,1-dioxide (**2b**). Spectroscopically (UV–VIS) and electrochemically (cyclic voltammetry) measured equilibrium constants at 25.0°C are presented and discussed for the reaction of **1a** and **1b** with alcohols (methanol, *n*-propanol, *n*-butanol, isobutanol, 2-propanol, **sec-butanol**, tert-butanol, ethylene glycol, allyl alcohol and 2-phenylethanol). A reaction of 1-propanethiol with **1c** was observed, but the alcohols did not react with **1c**, **1d** or the thiadiazolines (**2a**, **2b**). The effect of the solvent on the equilibrium constant of the 1a–ethanol system was measured using, besides acetonitrile, propylene carbonate, *N,N*-dimethylformamide, *N,N*-dimethylacetamide, dimethyl sulfoxide and tert-butanol. The results were correlated with an empirical H-bond acceptor solvent parameter. Previously unreported spectroscopic (UV–VIS, IR, ¹H and ¹³C NMR) data for some of the compounds studied are also provided. Copyright © 2000 John Wiley & Sons, Ltd.

KEYWORDS: 1,2,5-thiadiazoles; organic electrochemistry; nucleophilic addition; structure; reactivity

INTRODUCTION

Several derivatives including the thiadiazole ring have received considerable attention owing to their actual or potential applications in pharmacology and biology. A large number of bioactive molecules include this moiety. An important recent example is the discovery of 1,2,5-thiadiazole derivatives that are potent and specific inhibitors of HIV-1 inverse transcriptase.¹ Regarding specifically the 1,1-dioxide derivatives of 1,2,5-thiadiazole, antagonists of the H₂ receptors of histamine,^{2–6} antihypertensive drugs^{7–9} and central nervous system depressors¹⁰ were developed. In addition, some β-lactamic antibiotics,¹¹ quinazolinic cardiac stimulants,¹² anti-parasitical nitroimidazoles^{13,14} and pesticides¹⁵ are derivatives of 1,2,5-thiadiazoline 1,1-dioxides.

As a part of our electrochemical work on thiadiazoles, we have recently reported^{16–18} that ethanol (EtOH) adds

reversibly to 3,4-diphenyl- (**1a**; Scheme 1) or to 3-methyl-4-phenyl-1,2,5-thiadiazole 1,1-dioxide (**1b**) in a 1:1 molar ratio to give the corresponding 1,2,5-thiadiazoline 1,1-dioxides [4-ethoxy- 3,4-diphenyl (**2a**.EtOH) and 4-ethoxy-4-methyl-3-phenyl (**2b**.EtOH)].

These studies were extended in this work to other 1,2,5-thiadiazole 1,1-dioxide derivatives [**1a**, **1b**, phenanthro[9,10-*c*]- (**1c**) and acenaphtho[1,2-*c*]-1,2,5-thiadiazole 1,1-dioxide (**1d**), 3,4-diphenyl- (**2a**) and 4-ethoxy-5-methyl-3,4-diphenyl-1,2,5-thiadiazoline 1,1-dioxide (**2b**)] and to several nucleophiles (alcohols of different structural characteristics and propanethiol). Depending on the nucleophile–substrate combination, it was found that the addition reaction either did not take place, reached an equilibrium or was complete. The magnitude of the equilibrium constants, $K[\text{T},\text{N}]$ (T = thiadiazole derivative; N = nucleophile), the absence of reaction or its practical irreversibility were correlated with both nucleophile and substrate structure.

The nucleophiles used were methanol (MeOH), ethanol (EtOH), *n*-propanol (*n*-PrOH), *n*-butanol (*n*-BuOH), isobutanol (*i*-BuOH), 2-propanol (*i*-PrOH), *sec*-butanol (*s*-BuOH), *tert*-butanol (*t*-BuOH), ethylene glycol [ET(OH)₂], allyl alcohol (allylOH), 2-phenylethanol (2PhEtOH) and 1-propanethiol (PrSH).

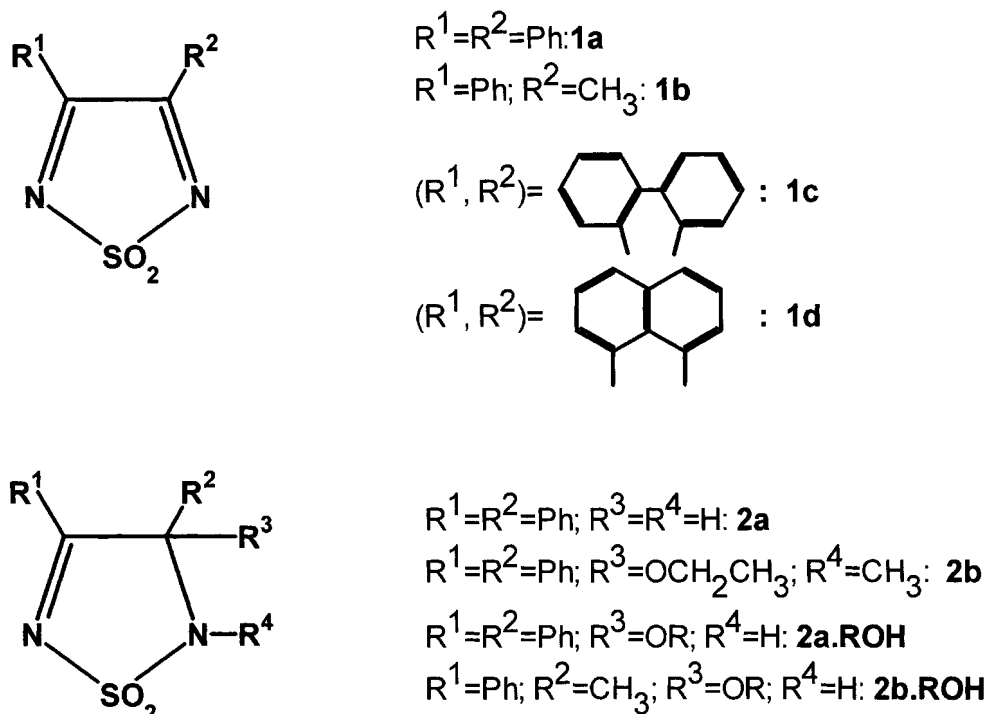
*Correspondence to: E. J. Vasini, INIFTA, Universidad Nacional de La Plata, C.C. 16, Suc. 4, (1900) La Plata, Argentina.

E-mail: vasini@inifta.unlp.edu.ar

Contract/grant sponsor: Consejo Nacional de Investigaciones Científicas y Técnicas (CONICET).

Contract/grant sponsor: Comisión de Investigaciones Científicas de la Provincia de Buenos Aires.

Contract/grant sponsor: Universidad Nacional de La Plata.



Scheme 1

Acetonitrile (ACN) was used as the solvent in most experiments. The equilibrium constant of the addition reaction of EtOH to **1a** was also studied in other solvents ($K[\mathbf{1a}, \text{EtOH}, \text{solvent}]$). Several aprotic solvents besides ACN were employed: propylene carbonate (PC), *N,N*-dimethylformamide (DMF), *N,N*-dimethylacetamide (DMA) and dimethyl sulfoxide (DMSO). The protic but non-reactive (see Results) solvent *t*-BuOH was also used.

The $K[\text{T}, \text{N}]$ values measured by either spectroscopic or voltammetric methods were in good agreement. The voltammetrically measured $K[\text{T}, \text{N}]$ depends on the reaction mechanism at the interface, proposed according to the experimentally observed electrochemical behavior. In contrast, spectroscopic absorbances are proportional to actual concentrations. Thus, the agreement reinforces the adequacy of the voltammetric mechanism.

EXPERIMENTAL

Synthesis and purification procedures

Thiadiazole derivatives. Compounds **1a**, **1b**, **1c**, **1d** and **2a** were synthesized, purified and characterized according to standard methods¹⁹ and **2b** was synthesized according to the reported technique.³ The purification procedure for **1b** was slightly modified by the addition of dry trifluoroacetic acid to the recrystallization solvent. Only after this change could the relatively low (29%) yields reported in the literature be achieved. The acid medium prevents a dimerization reaction of **1b** (see

Results). Crude samples of the **2a.ROH** and **2b.ROH** thiadiazoline compounds were isolated for all ROH, except *t*-BuOH, through evaporation of the solvent at reduced pressure (1–10 Torr) and room temperature from solutions of **1a** or **1b** in pure ROH.

Solvents and nucleophilic reactants. Standard methods.^{20–22} were used for the purification of commercial solvents, which were dried with molecular sieves and stored under a dry nitrogen atmosphere. Their water content was measured by Karl Fischer titration. As described below, the solutions of **1b** in ACN solvent are affected by the presence of water, even at very low concentrations. To observe this influence, two procedures were used to dry ACN: procedure *i* consisted in distillation over CaH_2 under a dry N_2 atmosphere and procedure *ii* consisted in further drying the distilled ACN through passage over activated 4A molecular sieves. ACN containing 350 ppm of water was obtained by means of procedure *i*, while procedure *ii* reduced the water content to 50 ppm.

Spectroscopic properties

1a. The UV spectra in several aprotic solvents and the ¹³C NMR in deuterated tetrahydrofuran have already been described.¹⁶

1b. UV: $\epsilon_{\text{max}} = 6.09 \times 10^3 \text{ l mol}^{-1} \text{ cm}^{-1}$ at 312 nm in dry ACN solution. ¹H NMR (δ , TMS) in ACN-*d*₃ solution:

phenyl multiplet (7.52–7.96 ppm), CH₃ singlet (2.67 ppm). ¹³C NMR (same solution): 170.5 ppm (Ph—C=N—), 167.5 ppm (CH₃—C=N—), four signals 134.0–127.7 ppm (phenyl ring) and 18.3 ppm (CH₃).

1c. UV (ACN or EtOH solvent): several absorption bands centered at 220 nm ($\epsilon = 4.77 \times 10^4$), 264 nm ($\epsilon = 3.86 \times 10^4$), 344 nm ($\epsilon = 1.39 \times 10^4$) and 454 nm ($\epsilon = 1.40 \times 10^3$ l mol⁻¹ cm⁻¹).

1d. UV (ACN or EtOH solvent): several absorption bands centered at 229 nm ($\epsilon = 6.27 \times 10^4$), 265 nm ($\epsilon = 2.48 \times 10^4$), 318 nm ($\epsilon = 7.38 \times 10^3$) and 333 nm ($\epsilon = 6.80 \times 10^3$ l mol⁻¹ cm⁻¹).

Compounds **1a** and **1b** in solutions of reactive alcohols are in the form of their ROH addition products: thiadiazolines **2a.ROH** and **2b.ROH** (Scheme 1). The ¹³C NMR spectrum of **2a.EtOH** has been published¹⁶. UV data (λ_{\max} and ϵ_{\max}) for several **2a.ROH** and **2b.ROH** are given in Table 3.

The ¹H NMR spectrum of **2b.MeOH** (in MeOH-*d*₄ solution) presents a multiplet at 7.46–8.33 ppm (phenyl) and a singlet at 1.80 ppm (—C—CH₃). The ¹³C NMR spectrum (same solvent) presents signals at 178.7 (Ph—C), 98.4 (CH₃—C—OMe) and ca 130 ppm (Ph). The methyl carbon resonance was observed at 26.5 ppm.

IR (KBr pellets): **2a.ROH** and **2b.ROH** obtained from the evaporation at room temperature and reduced pressure of solutions of **1a** or **1b** in ROH presented, in addition to IR absorptions from the RO groups and the phenyl substituent(s), sharp N—H stretching bands at ca 3300, 1560 (C=N), 1050 (C—N), 1315 and 1175 cm⁻¹ (>SO₂).

Experimental measurements

UV spectral measurements were made with a Cary 3 or a Zeiss PMQ3 spectrophotometer equipped with thermostated cell holders. Teflon-stoppered quartz cells of 1 cm optical pathlength were used. Molar absorptivities (ϵ) reported are accurate to $\pm 2.5\%$.

¹H and ¹³C NMR spectra were measured with a Bruker 200 MHz instrument and IR spectra with a Shimadzu IR-435 spectrophotometer.

The reaction of the thiadiazole substrates with nucleophiles was followed by the UV spectral changes that took place when a stock solution of one of the substrates (which will be designated generically as **T**) in ACN was added to a mixed ACN–nucleophile (usually ROH) solution: the UV absorption band of **T** gradually decreased in intensity and an absorption band (corresponding to the thiadiazoline addition product, **T.ROH**) appeared and increased in intensity. Isosbestic points were observed during these changes (usually ca 240 and 290 nm). The rate of change of the absorbance was faster the higher the alcohol concentration and an equilibrium

spectrum was finally obtained. The relative decrease (increase) in absorbance of the **T** (**T.ROH**) band was larger the higher the molar ROH concentration. The equilibrium constant ($K[\mathbf{T},\text{ROH}]$) was calculated using a Benesi–Hildebrand-type equation:¹⁶

$$\frac{[\text{ROH}][\mathbf{T}]_0}{A_{\mathbf{T},\text{ROH}}^{\lambda_1}} = \frac{1}{K[\mathbf{T},\text{ROH}]\epsilon_{\mathbf{T},\text{ROH}}^{\lambda_1}} + \frac{[\text{ROH}]}{\epsilon_{\mathbf{T},\text{ROH}}^{\lambda_1}} \quad (1)$$

where λ_1 and $\epsilon_{\mathbf{T},\text{ROH}}^{\lambda_1}$ are the wavelength of maximum absorption and the corresponding molar absorptivity of **T.ROH**, and

$$A_{\mathbf{T},\text{ROH}}^{\lambda_1} = A_{\text{exp}}^{\lambda_1} - \epsilon_{\mathbf{T}}^{\lambda_1} \times \frac{A_{\text{exp}}^{\lambda_2}}{\epsilon_{\mathbf{T}}^{\lambda_2}} \quad (2)$$

is the absorbance of **T.ROH** at λ_1 , corrected for the absorbance of **T** at the same wavelength (λ_2 and $\epsilon_{\mathbf{T}}^{\lambda_2}$ are the wavelength of maximum absorption and the corresponding molar absorptivity of **T**). Under our experimental conditions, the nucleophile concentration remained virtually constant ($[\text{ROH}]_t = [\text{ROH}]_0$) because the initial concentration of ROH was always much higher than $[\mathbf{T}]_0$.

According to the criteria proposed by Person²³ to minimize errors, the equilibrium constants were measured for conditions under which the equilibrium concentration ratio, $[\mathbf{T}]/[\mathbf{T},\text{ROH}]$, ranged between 0.1 and 10. The coherency of the experimental points was tested according to the method of Rose and Drago.²⁴

Cyclic voltammetric (CV) experiments were performed in a conventional undivided gas-tight glass cell with dry nitrogen gas inlet and outlet. The working electrode was a 3 mm diameter vitreous carbon disk encapsulated in Teflon, the counter-electrode was a 2 cm² Pt foil and an Ag⁺ (0.1 M, ACN)/Ag reference electrode (to which all potentials reported are referred) was used. The supporting electrolyte was 0.25 M NaClO₄. An LYP-M2 potentiostat, a three-module LYP sweep generator and a Houston Omnigraphic 2000 pen recorder were used.

The voltammetric behavior of **1a** and **1b** in ROH–ACN mixed solvent solutions was similar to that reported for the **1a**–EtOH–ACN system:^{17,18} before the addition of ROH, the ACN solution of thiadiazole (**T**) showed two reversible voltammetric signals corresponding to the **T**[•]/**T**^{•-} (peak I) and the **T**⁻/**T**²⁻ (peak II) couples [see Fig. 2(1a), curve 1]. The addition of ROH produced no immediate changes, but the voltammograms started to change with time at a rate that increased with the amount of ROH added. The second cathodic peak decreased in current intensity and disappeared from the final equilibrium voltammograms for all experimental ROH concentrations used. The current intensity of the first cathodic peak also decreased and reached a final equilibrium intensity that depended

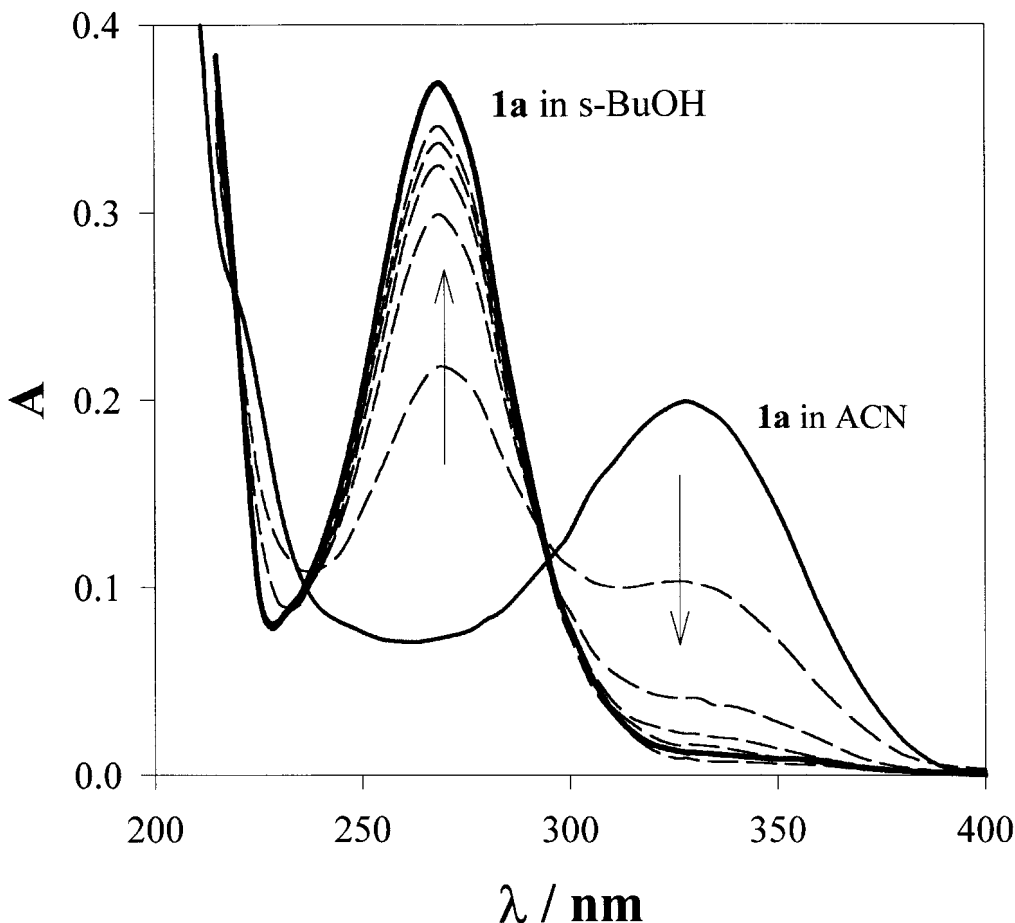


Figure 1. UV-visible spectra of the **1a**–s-BuOH–ACN system at different times (*t*) after addition of a solution of s-BuOH in ACN to solution of **1a** in ACN. Analytical concentrations: [**1a**] = 2.35×10^{-5} M, [s-BuOH] = 12.83 M. *T* = 25.0 °C. Full lines correspond to the spectrum of **1a** in the pure solvents indicated. Dotted lines correspond to spectra at *t* = 7.5, 29, 49, 69 and 120 h after s-BuOH addition. The direction of absorbance change with increasing time is indicated by the arrows

inversely on the ROH concentration. Two cathodic peaks [IIIc and IVc; see Fig. 2(1a), curve 2] appeared at lower potentials.

According to the proposed¹⁷ mechanism, equal quantities of **T** and **T·ROH** are consumed at peak Ic (provided that peak IIc has already disappeared), and the cathodic peaks (IIIc and IVc) are related to the electroreduction of the remaining **T·ROH**. A function [Eqn. (3)] of the relative intensity of these peaks and the voltage sweep rate (*v*) can be used to calculate the equilibrium constant:

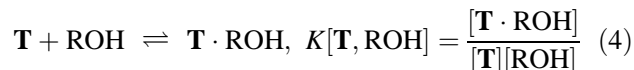
$$K[\mathbf{T}, \text{ROH}][\text{ROH}] = \frac{2 \left[\frac{i(\text{IIIc})}{v^{1/2}} + \frac{i(\text{Ic})}{2v^{1/2}} \right]}{\frac{i(\text{Ic})}{v^{1/2}}} \quad (3)$$

The preparation of solutions, the CV experiments and other manipulations were carried out in a glove-box under a dry nitrogen atmosphere.

RESULTS

Spectroscopic (UV) and electrochemical (CV) behavior of the reacting substrate–nucleophile systems. Comments on the kinetic behavior

The nucleophilic addition reaction



can be monitored (see Experimental section) by the changes as a function of time in the UV spectra (Fig. 1) or in the cyclic voltammograms (Fig. 2) of the **T**–ROH–solvent systems.

The equilibrium constants measured for all reacting systems by both methods are given in Table 3 and will be commented on below. Some comments on the effect of the residual (50–350 ppm, see Experimental section)

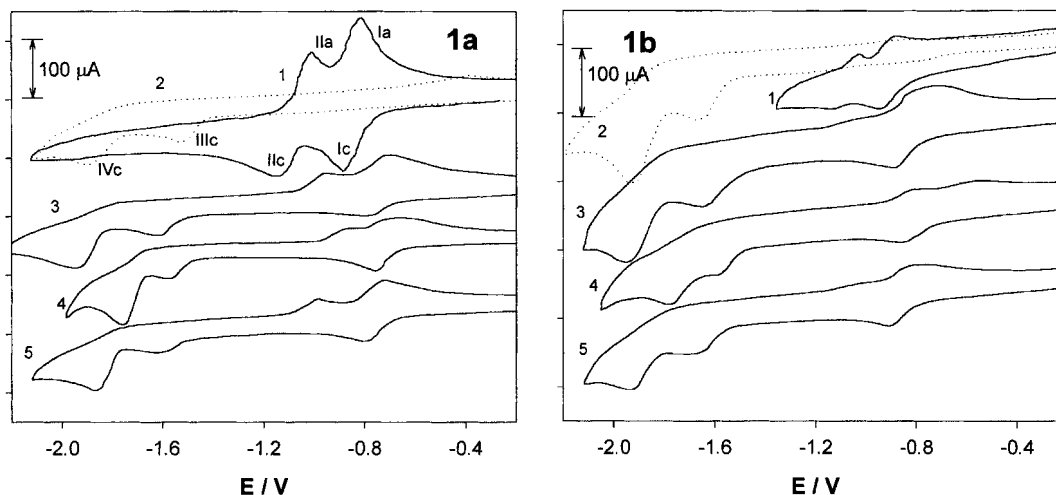


Figure 2. Cyclic voltammograms of **1a** and **1b** in ACN and EtOH solvents and equilibrium voltammograms in several ROH-ACN solvent mixtures. Supporting electrolyte, 0.25 M NaClO₄, vitreous carbon disk working electrode. Part (1a): scan rate = 0.1 V s⁻¹. Curve 1, [**1a**] = 1.51 mM, ACN solvent; curve 2 (dotted line), [**1a**] = 3.16 mM, EtOH solvent; curve 3, [**1a**] = 4.2 mM in 1.49 M *n*-butanol in ACN; curve 4, [**1a**] = 4.2 mM in 2.20 M ethylene glycol in ACN; curve 5, [**1a**] = 4.2 mM in 2.66 M allyl alcohol in ACN. Part (1b): scan rate = 0.2 V s⁻¹. Curve 1, [**1b**] = 1.06 mM, ACN solvent; curve 2 (dotted line), [**1b**] = 5.05 mM, EtOH solvent; curve 3, [**1b**] = 3.70 mM in 2.19 M isobutanol in ACN; curve 4, [**1b**] = 3.73 mM in 4.74 M ethylene glycol in ACN; curve 5, [**1b**] = 3.65 mM in 2.03 M *n*-propanol in ACN

water content of the solvent and nucleophilic reactants may be useful here.

Residual water and reaction kinetics. Detailed absorbance vs time measurements were made in many experiments to investigate the kinetics of the reaction. The evolution of all reacting systems fitted a pseudo-first-order law, but the calculated rate constants (k_{obs}) depended strongly on the water content of the solvent¹⁶ (Table 1). A comparison of the first row of Table 1 with the last three rows shows that a water content of 350 ppm results in a k_{obs} value which is ca 40 times higher than the minimum obtained by decreasing the water content or the water activity by protonation (TFA addition) or complexation with acid cations (addition of Li⁺).

Table 1. Pseudo-first-order rate constant, k_{obs} , for the addition of EtOH to **1a** in ACN solution for different ACN purification procedures^a

H ₂ O content of ACN (ppm)	[TFA]/[1a]	[LiClO ₄](M)	k_{obs} (h ⁻¹)
350 (i)	—	—	7.8 ± 0.2
50 (ii)	—	—	2.48 ± 0.04
350 (i)	3.02	—	0.99 ± 0.01
50 (ii)	3.02	—	0.20 ± 0.01
350 (i)	100	—	0.19 ± 0.01
350 (i)	—	0.107	0.20 ± 0.01

^a[EtOH] = 6.50 M; [**1a**] = 8.94 × 10⁻⁵ M; T = 25.0 °C. The water content of ACN (Karl Fischer titration) was measured after the following pretreatments: *i* = fractional distillation over CaH₂, N₂ atmosphere; *ii* = fractional distillation over CaH₂ in an N₂ atmosphere, followed by drying with 4 Å molecular sieves.

Water addition to, for example, **1a** (which is the first step in the hydrolysis reaction²⁵) must be very similar to EtOH addition. The resulting thiadiazoline (**2a**.HOH), has a UV absorption spectrum¹⁶ similar to that of **2a**.EtOH. Hence the observed rate corresponds to the sum of both water and EtOH addition reactions. The results imply that H₂O adds much faster than EtOH and that the water (or EtOH) addition reaction is not catalyzed by acids. Beyond a certain minimum and up to the maximum experimentally employed, the molar ratio [TFA]/[**1a**] did not affect the measured k_{obs} (Table 1, fourth and fifth rows). This was also found to apply to **1b** (Table 2).

Residual water and equilibrium constants. The $K[\text{T},\text{ROH}]$ values are not measurably affected by residual water, e.g. the values of $K[\text{1a},\text{EtOH}]$ and $K[\text{1b},\text{EtOH}]$, that were calculated when the kinetic runs included in Tables 1 and 2 reached equilibrium, agreed within the experimental error. This is reasonable since the ROH to

Table 2. Pseudo-first-order rate constants for addition reaction of EtOH to **1b** in ACN solution for different dry TFA concentrations^a

[1b] (M × 10 ⁴)	[TFA]/[1b]	k_{obs} (h ⁻¹)
1.559	0.802	0.117 ± 0.007
1.559	11.26	0.119 ± 0.007
1.547	123.3	0.118 ± 0.003
1.313	130.6	0.116 ± 0.007

^a[EtOH] = 2.67 M; T = 25.0 °C. ACN purification procedure: *ii* (Table 1).

Table 3. Spectrophotometrically (UV) and voltammetrically (CV) measured equilibrium constants $K[\mathbf{T}, \text{ROH}]$ [reaction (4)], Benesi–Hildebrand [Eqn. (1)] and gravimetric extinction coefficients ($\epsilon_{\text{BH}}^{\lambda}$ and $\epsilon_{\text{grav}}^{\lambda}$) for the addition products ($\mathbf{T} \cdot \text{ROH}$)^a

T	ROH	$\epsilon_{\text{BH}}^{\lambda} \times 10^3$ ($\text{l mol}^{-1} \text{cm}^{-1}$)	$\epsilon_{\text{grav}}^{\lambda} \times 10^3$ ($\text{l mol}^{-1} \text{cm}^{-1}$)	$K[\mathbf{T}, \text{ROH}]$ (l mol^{-1})	
				UV	CV
1a	MeOH	16.2 ± 0.2	15.6 ± 0.5	3.6 ± 0.1	—
	EtOH	16.8 ± 0.3	16.4 ± 0.8	3.3 ± 0.2	3.2 ± 0.2
	EtOH	15.5 ± 0.1	—	3.6 ± 0.5 ^a	—
	n-PrOH	14.1 ± 0.6	15.1 ± 0.4	3.7 ± 0.8	3.0 ± 0.1
	n-BuOH	16.5 ± 0.1	16.8 ± 0.4	3.5 ± 0.6	3.4 ± .02
	i-BuOH	17.1 ± 0.1	17.5 ± 0.3	2.8 ± 0.1	2.3 ± .1
	i-PrOH	19.4 ± 0.1	16.0 ± 0.3	0.26 ± 0.01	0.27 ± 0.02
	s-BuOH	22.2 ± 2.8	15.9 ± 0.3	0.21 ± 0.04	0.22 ± 0.02
	AllylOH	—	—	—	0.93 ± 0.01
	2PhEtOH	—	—	—	2.5 ± 0.1
	ET(OH) ₂	—	—	—	1.37 ± .02
1b	EtOH	—	14.7 ± 0.2	1.7 ± 0.2	1.5 ± .1
	EtOH	14.8 ± 0.2	—	1.4 ± 0.1 ^a	—
	n-PrOH	15.9 ± 0.4	14.5 ± 0.3	1.6 ± 0.2 ^a	1.7 ± .1
	n-BuOH	16.7 ± 0.5	14.1 ± 0.2	1.6 ± 0.1 ^a	2.1 ± .1
	i-BuOH	15.7 ± 0.5	—	1.4 ± 0.1 ^a	2.1 ± .1
	i-PrOH	24.0 ± 3.3	14.0 ± 0.3	0.09 ± 0.02 ^a	0.25 ± 0.02
	s-BuOH	14.7 ± 2.7	—	0.12 ± 0.03 ^a	0.22 ± 0.01
	ET(OH) ₂	—	—	—	0.75 ± 0.01

$\lambda = 268 \text{ nm}$ for **1a** and 265 nm for **1b** [see Eqn. (2)]. Indicated errors are least-squares standard deviations.

^aMeasurements made with the addition of TFA (see text).

water molar concentration ratio is so high (*ca* 10^5 – 10^6) that the interconversion reaction (5) should be shifted completely to the right:



The measurement of equilibrium constants for the addition of water to thiadiazoles is complicated by the subsequent hydrolysis reaction²⁵ which prevents the attainment of a stable equilibrium. However, an estimation of its value could be obtained using the voltammetric method in the **1a**–H₂O–DMSO system, in which the slowest hydrolysis rate was observed. Water concentrations in the range 0.1–0.2 M were used (i.e. 1800–3600 ppm). The $K[\mathbf{1a}, \text{HOH}]$ value obtained ($28 \pm 2 \text{ l mol}^{-1}$) was about three times $K[\mathbf{1a}, \text{EtOH}]$ in DMSO solution (Table 4).

In the case of **1b**, the water content and activity were reduced to a minimum to avoid the above-mentioned dimerization reaction. Therefore, most spectroscopic equilibrium measurements were made in the presence of added TFA (typically with a $[\text{TFA}]/[\mathbf{1b}]_0$ molar ratio of *ca* 0.8), but control experiments in very dry EtOH–ACN mixtures, without the addition of TFA, confirmed that the $K[\mathbf{1b}, \text{EtOH}]$ values did not change appreciably in the presence of TFA (Table 3). The addition of acid was not necessary in equilibrium voltammetric measurements owing to the presence of the supporting electrolyte, as commented upon below.

Residual water in ACN solutions of 1b. It was observed that, although ACN solutions of **1b** in freshly

purified and thoroughly dried solvent (procedure *ii*, Experimental section) remained unchanged for several hours, the intensity of the UV absorption band of **1b** at 312 nm decreased slowly in nominally dry ACN (procedure *i*, Experimental section). The rate of decrease was faster when a small amount of water was added to the ACN solvent. The decrease in the absorbance of the 312 nm band was accompanied by the appearance and increase of two new bands at *ca* 255 and 385 nm. Two isosbestic points at *ca* 282 and 350 nm were observed and the solution acquired a light yellow color. However, when fresh solutions of **1b** in dry ACN (procedure *i*), in which only the 312 nm band was observed in the UV spectrum, were analyzed by thin-layer chromatography (TLC), two spots were found. Apparently the silica of the TLC layer, the residual water present in the solvent or the water incorporated during the chromatographic run catalyzed the process of the development of the yellow color.

Stable UV spectra and a ‘single spot’ (the one

Table 4. $K[\mathbf{1a}, \text{EtOH}]$ measured in several solvents at 25.0 °C and empirical H-bond acceptor solvent parameters^a

Solvent	β	DN	$K[\mathbf{1a}, \text{EtOH}]$ (l mol^{-1})
ACN	0.31	14.1	3.2 ± 0.2
PC	0.40	15.1	3.9 ± 0.1
DMF	0.69	26.6	12.9 ± 0.2
DMA	0.76	27.8	14.5 ± 0.4
DMSO	0.76	29.8	9.0 ± 0.7
t-BuOH	1.01	20.0	14.8 ± 0.7

^aLeast-squares fitting gives $\text{p}K = -1.36 \beta$ with a regression coefficient $r = 0.997$.

corresponding to the larger R_f value) TLC runs were obtained upon addition of dry TFA to solutions of **1b** in nominally dry ACN. Preliminary experiments indicated that dimerization of **1b** takes place in neutral or basic, nominally dry, ACN solutions and on the chromatographic plate. The added acid drastically decreases the reactivity of residual water (the acid cation of the supporting electrolyte has a similar effect, as mentioned below in the section on electrochemical measurements). The dimerization reaction of **1b** will be discussed elsewhere.

UV Spectrophotometric evaluation of equilibrium constants

Reaction (4) was followed spectroscopically, as described in the Experimental section, through the measurement of spectral changes such as those shown in Fig. 1.

This method was used for solutions of the thiadiazole substrates at 25.0°C in ROH solvents and in mixed ROH–ACN solvents. Spectral changes similar to those described above were observed for **1a** and **1b** in all ROH and ROH–ACN solvent mixtures employed, with the exception of *t*-BuOH, with which the substrates did not react, as evidenced by an unchanged UV spectrum over a 1 year period at 25.0°C. Similarly, no change in the spectra was observed during a period of several months for solutions of **1c**, **1d**, **2a** or **2b** in any of the ROH or ROH–ACN solvents.

The application of a Benesi–Hildebrand-type treatment [Eqns (1) and (2)], with $\lambda_1 = 268$ nm for **2a**.ROH and 265 nm for **2b**.ROH, and $\lambda_2 = 328$ nm for **1a** and 312 nm for **1b**, gave a good linear dependence with least-squares correlation coefficients better than 0.998 (4–9 values).

The Benesi–Hildebrand-calculated equilibrium constants and molar absorptivities (ϵ_{BH}) were compared with the molar absorptivities (ϵ_{grav}) calculated assuming that, in pure ROH solvents, the substrates were completely converted to the thiadiazolines (**2a**.ROH or **2b**.ROH). The differences between ϵ_{BH} and ϵ_{grav} (Table 3) are only significant (ϵ_{grav} being smaller) for the systems with smaller equilibrium constants, i.e. when the assumption made in measuring ϵ_{grav} was not correct.

The linearity of the Benesi–Hildebrand plots indicated a 1:1 reaction of **1a** or **1b** with all reactive alcohols, since monoaddition was one of the premises used to deduce Eqn. (1).

It must also be mentioned that the eventual double addition products would be saturated (thiadiazolidine) compounds. These have UV absorption maxima in the same region as the thiadiazolines, but their molar absorptivities are one order of magnitude smaller.¹⁶ Hence the experimental dispersion of the UV-measured equilibrium constant places an upper limit of ca 10% on

the eventual existence of double-addition products. Furthermore, no decreasing trend in the K values with increase in ROH concentration, which could suggest a contribution from double addition, was ever observed.

Voltammetry in ROH–ACN solvent mixtures. Voltammetric evaluation of equilibrium constants

The electrochemical properties of **1a** and **1b** in ROH–ACN mixed solvent solutions were studied using CV as described in the Experimental section and exemplified in Fig. 2.

The relation between the intensity of the voltammetric peaks and the equilibrium constant depends on the mechanism of the electrochemical and the homogeneous reactions at each peak. The mechanism found for the **1a**–EtOH–ACN system¹⁷ was also operative for the systems studied here, as was concluded from the very similar voltammetric responses. The voltammetric method, which can be used with UV-absorbing solvents or nucleophiles, is further supported by the agreement (Table 3) between the spectrophotometrically and the voltammetrically measured equilibrium constants.

The voltammetric $K[\text{T,ROH}]$ values given in Table 3 were obtained from the linear plots of the right-hand side of Eqn. (3) vs $[\text{ROH}]$ for different **T**–ROH–ACN systems. The errors reported are least-squares standard deviations of these plots.

It must be mentioned that no yellowing or decomposition was observed during the voltammetric measurement of the **1b**–ROH–ACN systems. The relatively high concentration of Na^+ from the supporting electrolyte was probably sufficient to decrease the activity of the residual water, thus inhibiting the decomposition reaction.

It can be recalled that thiadiazolidine compounds are electroinactive under the present experimental conditions.¹⁶ Here the practical absence of double addition could be deduced with the same argument as used above for the UV spectral measurements.

¹H and ¹³C NMR and IR characterization of the addition compounds

The characteristics of the spectra in ROH solvents (see Experimental section) are in agreement with the postulated addition reaction of alcohols to one of the C=N double bonds of the heterocycle. The downfield shift in the ¹³C NMR resonance of the methyl carbon of **2b**·MeOH (26.5 ppm) with respect to the corresponding methyl signal of **1b** (18.3 ppm) indicated, according to known additivity rules,²⁶ that the methoxy substituent had added to the heterocyclic carbon atom bearing the methyl substituent, since the addition to the 'phenyl' heterocyclic carbon would result in an upfield shift. This

confirms our indirect electrochemical results¹⁸ and theoretical calculations.²⁷

The IR spectrum of the solid residues obtained from the evaporation at room temperature and reduced pressure of solutions of **1a** or **1b** in all ROH (except *t*-BuOH) presented bands that closely resembled those of the corresponding thiaziazolines **2a** or **2b** (for instance, **2b** shows bands at 1590, 1560, 1490, 1450, 1325, 1170 and 1045 cm^{-1}). The sharpness of the band at ca 3300 cm^{-1} and its persistence under prolonged vacuum at room temperature indicated that it was an N–H band, and did not originate from residual alcohol in the solid. Further vacuum drying of the compounds at higher temperature (60 °C) for several days gave solids with an IR spectrum identical with that of the initial thiaziazole compound (**1a** or **1b**). As *t*-BuOH does not react, only **1a** or **1b** was recovered from room temperature and reduced pressure evaporation of solutions of **1a** or **1b** in *t*-BuOH.

Influence of the solvent in the **1a**–EtOH equilibrium

The influence of the solvent in the voltammetric behavior of **1a** was analyzed in PC, DMF, DMA and DMSO, in addition to ACN. The effect of the solvent on the nucleophilic addition reaction [Eqn. (4)] was evaluated in mixtures of these solvents with EtOH at 25.0 °C. Since *t*-BuOH does not react, it was also used as a test solvent. The behavior of the **1a**–EtOH–*t*-BuOH system was investigated using the UV spectrophotometric method, because *t*-BuOH is not an adequate electrochemical solvent.

For the **1a**–solvent systems, two one-electron voltammetrically reversible couples, similar to those shown for the initial voltammogram in Fig. 2, were observed in all the solvents investigated. The potential of peak Ic did not change appreciably with the change of solvent, whereas that of peak IIc shifted to lower potentials with an increase in the donor number (DN) of the solvent. The effect is undoubtedly caused by the decrease in the Lewis acidity of the supporting electrolyte cation in more basic solvents.¹⁷

The values of $K[\mathbf{1a}, \text{EtOH}]$ in different solvents are given in Table 4. As expected, they correlate well with the empirical hydrogen bond acceptor β parameter of the solvent²⁸ (least-squares fit: $\text{p}K = -1.36\beta$, $r = 0.997$, six points).

As detailed above an equilibrium constant for the addition of water to **1a** was voltammetrically estimated using the **1a**–H₂O system in DMSO solution.

Voltammetric study of the PrSH addition to thiaziazoles in ACN

The voltammetric behavior of the **1a**–PrSH system in

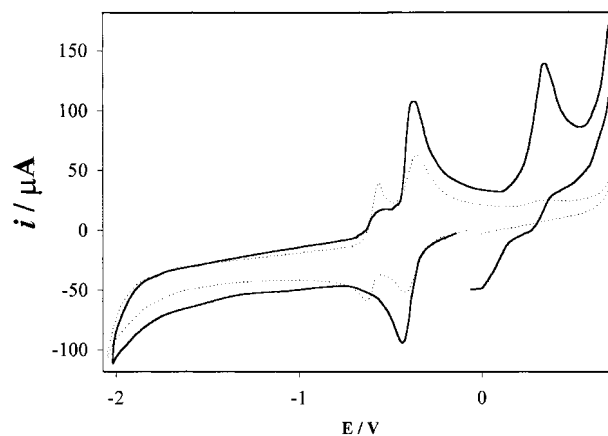


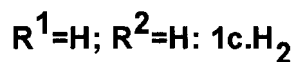
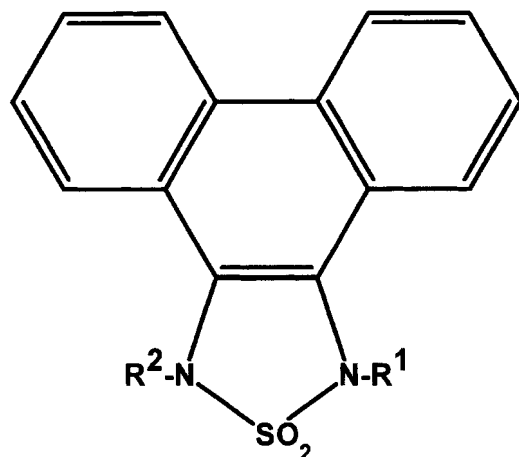
Figure 3. Cyclic voltammograms of the **1c**–PrSH–ACN system. [**1c**] = 2.95 mM; [PrSH] = 0.859 M; $\nu = 0.2 \text{ V s}^{-1}$. (Dotted line, after solution preparation; solid line, 30 days after solution preparation)

ACN solution was similar to those of the reactive **1a**–ROH systems. The time sequence and the magnitude of the changes in the current intensity of the voltammetric peaks were nearly identical, although the peaks identified as IIIc and IVc appeared at somewhat higher potentials (ca –1.45 and –1.75 V, respectively) than those of the **1a**–ROH systems.

It was found that a 0.17 M concentration of PrSH was sufficient to drive the equilibrium position so far to the right that the reaction could be considered complete. At those low nucleophile concentrations, the equilibration time was more than 3 months. After that period, the intensity of peak Ic was too small to measure an equilibrium constant accurately, but it could be estimated as larger than 300 l mol^{-1} .

The voltammetric response of **1c** in ACN solution in the presence of added PrSH differed from that of **1a** under the same conditions: the two couples of the **1c**–ACN system ($E_p[\mathbf{1c}/\mathbf{1c}^-] = -0.58 \text{ V}$; $E_p[\mathbf{1c}^-/\mathbf{1c}^{2-}] = -0.73 \text{ V}$) were observed in freshly prepared **1c**–PrSH–ACN solutions (Fig. 3, dotted line). A slow decrease in the current intensity of the second couple and an increase in the first were observed during a few days. The voltammogram shown in Fig. 3 (full line) was finally obtained: the first couple has doubled its current intensity and shows reversible behavior, the second couple has practically disappeared and no further cathodic peaks (corresponding to IIIc and IVc) have developed. An anodic peak at 0.44 V also observed.

A solid was obtained by evaporation (at room temperature and reduced pressure) of the solvent from solutions that presented the above-described voltammetric behavior. The IR spectrum (KBr pellet) of the solid had, besides absorptions corresponding to **1c**, other bands that were similar in position and intensity to those of the recently synthesized thiaziazoline of **1c**²⁹ (**1c**H₂; Scheme 2): a low-intensity doublet at 1635 and



Scheme 2

1610 cm^{-1} which corresponds to 9,10-disubstituted phenanthrenes (1640 and 1608 cm^{-1} in $\mathbf{1c.H}_2$) and an intense band at 1280 cm^{-1} ($\mathbf{1c.H}_2$: 1275 cm^{-1}) assigned to the C–N stretching in the >C=C-N< group. IR bands at 3300 (NH), 2920 (CH aliphatic) and 1370 cm^{-1} (CH_3) were also observed. The anodic peak at 0.44 V is also observed in the voltammogram of $\mathbf{1c.H}_2$.²⁹

Hence the product of the addition of PrSH to $\mathbf{1c}$ ($\mathbf{1c.PrSH}$; Scheme 2) might reasonably be considered an *N*-propylthio derivative. As discussed in the case of $\mathbf{1c.H}_2$, the *N,N*-addition compound is stabilized by the resonance energy of a phenanthrene hydrocarbon ring that would not be available had PrSH added to a C=N double bond. Compound $\mathbf{1c.PrSH}$, as $\mathbf{1c.H}_2$, was unstable and could not be isolated. It reverted easily to $\mathbf{1c}$ during purification treatments.

DISCUSSION

Monoaddition

Reactive alcohols add to thiadiazoles $\mathbf{1a}$ and $\mathbf{1b}$ in a 1:1 molar ratio. Although the molecules present two similar (or identical, in the case of $\mathbf{1a}$) sites for the addition reaction, the addition of one molecule of nucleophile seems to decrease the reactivity of the remaining reaction site of the substrate. No reaction with ROH nucleophiles or PrSH was observed with thiadiazolines, such as the $\mathbf{2a}$ and $\mathbf{2b}$, that have only one C=N bond in the heterocycle ring.

Monoaddition is independently supported by all

experimental techniques employed. This decrease in reactivity after the first addition has also been observed recently and used to obtain selectively monoaddition products from the reaction of $\mathbf{1a}$ with Grignard reagents.³⁰ This behavior was qualified as ‘an interesting feature’, without further comments on its cause.

According to our structural studies of these molecules,²⁷ the mutual steric hindrance of the $\mathbf{1a}$ phenyl substituents causes them to rotate out of coplanarity with the heterocyclic plane (to a phenyl–heterocycle dihedral angle of ca 43°). We have also shown that the interaction between the methyl and the phenyl substituents in $\mathbf{1b}$ has similar steric effects. The phenyl–heterocycle dihedral angle in $\mathbf{1b}$ is ca 41°. Thus, the resonance interaction between the C=N bond(s) and the phenyl ring(s) can only take place to a small extent.

Upon monoaddition, the heterocyclic carbon atom of $\mathbf{1a}$ that had bonded to the nucleophile changes from sp^2 to sp^3 hybridization, and the corresponding phenyl substituent is displaced out of the crowded region over the C–C bond of the heterocycle. This frees the phenyl substituent on the other heterocyclic carbon to rotate to coplanarity and full delocalization interaction of its π -system with the corresponding C=N double bond can take place. This remaining Ph–C=N– group turns into a typical (coplanar and comparatively less reactive) aromatic imine. The addition of a nucleophile to the ‘methyl side’ of a $\mathbf{1b}$ molecule has similar effects.

This thiadiazoline geometry has been confirmed by x-ray monocrystalline diffraction studies of $\mathbf{2a}$ and $\mathbf{2b}$.³¹ The measured phenyl–heterocycle dihedral angles for the sp^3 and the sp^2 sides of these molecules were 89.23° (sp^3 ; $\mathbf{2a}$), 96.58° (sp^3 ; $\mathbf{2b}$), 7.6° (sp^2 ; $\mathbf{2a}$) and 10.7° (sp^2 ; $\mathbf{2b}$).

Equilibrium constant values. Dependence on the structure of nucleophile and substrate

The experimentally measured $K[\mathbf{1a,ROH}]$ and $K[\mathbf{1b,ROH}]$ for all saturated, linear-chain, primary alcohols (Table 3) average 3.4 ± 0.2 and 1.7 ± 0.2 , respectively. Thus, as in the case of ROH addition to the carbonyl group,³² there is no measurable steric effect caused by the length of the hydrocarbon chain.

The sites for the nucleophilic attack are, of course, different in $\mathbf{1a}$ and $\mathbf{1b}$ molecules [Ph–C(C)=N– or $\text{CH}_3\text{—C(C)=N—}$, respectively), but in both cases the reaction involves the breaking and formation of similar bonds and similar structural changes. The experimental fact that $K[\mathbf{1a,ROH}] \approx 2K[\mathbf{1b,ROH}]$ for sterically unhindered alcohols might indicate that the different reaction sites are of secondary importance and that the factor of 2 in the K values is statistically determined: $\mathbf{1a}$ provides two possibilities for the bonding of a ROH molecule whereas $\mathbf{1b}$ has only one.³³

A steric effect due to differences in the reaction sites of the substrates can be observed when the K values for

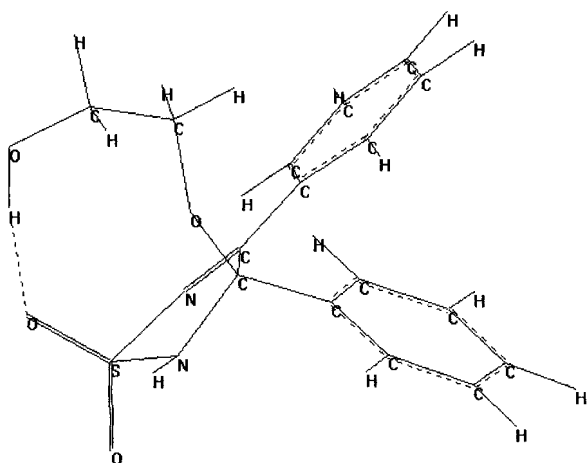


Figure 4. Optimized geometry (PM3 semiempirical method) for the adduct of ethylene glycol and **1a** [**1a**·ET(OH)₂]. The length of the hydrogen bond (dotted line) is 1.84 Å

linear-chain nucleophiles are compared with those corresponding to β -branched ROH nucleophiles (Table 3). $K[\mathbf{1a}, \beta\text{-branched ROH}]$ is ca 30% smaller than the 3.4 l mol⁻¹ value of $K[\mathbf{1a}, \text{linear-chain ROH}]$ ($K[\mathbf{1a}, i\text{-BuOH}] \approx K[\mathbf{1a}, 2\text{PhEtOH}] \approx 2.4$ l mol⁻¹), while $K[\mathbf{1b}, i\text{-BuOH}] \approx 1.7$ l mol⁻¹ $\approx K[\mathbf{1b}, \text{linear-chain ROH}]$.

Steric hindrance caused by the structure of the nucleophile must be the dominant effect for secondary and tertiary alcohols. The equilibrium constants for the addition of *i*-PrOH or *s*-BuOH are of comparable magnitude for both substrates, but ca 10 times smaller than the 'linear-chain ROH' value. No reaction was observed between either substrate and *t*-BuOH.

AllylOH and ET(OH)₂ should, in what refers to steric effects, be similar to *n*-PrOH. The equilibrium constant values should therefore be ordered according to the inductive effect [i.e. *n*-PrOH > AllylOH > ET(OH)₂]. However, K values for the reaction with **1a** were approximately 3.3, 0.9 and 1.4 l mol⁻¹, respectively. The discrepant high value for ET(OH)₂ might be related to the ability of the resulting thiadiazoline to form an H-bonded ring, such as that depicted in Fig. 4, obtained by a geometry optimization with a semiempirical (PM3) method.

The lack of addition of alcohols to **1c** and **1d** must be related to the smaller electropositive character of the heterocyclic carbon atoms of these substrates due to the charge dispersal possibilities of their π -system, which, besides being larger than those of **1a** or **1b**, are also coplanar with the heterocycle.²⁷ A much stronger nucleophile, such as PrSH, which reacts practically irreversibly with **1a**, is necessary to observe addition reactions to **1c**. The resulting thiadiazoline, however, is structurally different (Scheme 2).

Although a relatively small number of different solvents could be used, the good single-parameter correlation between the pK values for the reaction of **1a**

with EtOH and the solvent hydrogen bond acceptor parameter β is in agreement with the characteristics of reaction (4).

Acknowledgements

This work was financially supported by the Consejo Nacional de Investigaciones Científicas Y Técnicas (CONICET), the Comisión de Investigaciones Científicas de la Provincia de Buenos Aires (CIC Pcia. Bs. As.) and the Universidad Nacional de La Plata (UNLP), Facultad de Ciencias Exactas, Departamento de Química and Facultad de Ingeniería, Departamento de Ingeniería Química. M.V.M and J.A.C. are researchers of CONICET and UNLP and S.L.A. and E.J.V. are researchers of CIC Pcia. Bs. As. and UNLP. The authors acknowledge Professor Dr E. G. Gros (UMyMFOR, Universidad de Buenos Aires, CONICET) for analytical and spectroscopic measurements and Professor O. Piro (Departamento de Física, Facultad de Ciencias Exactas UNLP) for x-ray diffraction measurements.

REFERENCES

- Hanasaki Y, Watanabe H, Katsuura K, Takayama H, Shirakawa S, Yamaguchi K, Sakai S, Ijichi K, Fujiwara M, Konno K, Yokota T, Shigeta S, Baba M. *J. Med. Chem.* 1995; **38**: 2038.
- Lumma WC, Jr, Anderson PS, Baldwin JJ, Bolhofer WA, Habecker CH, Hirsfield JM, Pietruszkiewicz AM, Randall WC, Torchiana ML, Britcher SF, Clineschmidt BV, Denny GH, Hirschmann R, Hoffman JM, Phillips BT, Streeter KB. *J. Med. Chem.* 1982; **25**: 207.
- Algieri AA, Luke GM, Standridge RT, Brown M, Partyka RA, Crenshaw RR. *J. Med. Chem.* 1982; **25**: 210.
- Baldwin JJ, Bolhofer WA, Lumma WC, Jr, Amato JS, Karady S, Weinstock LM. Eur. Pat. 40696 (1981); CA 1981; **96**: 85598.
- Crenshaw RR, Algieri AA. US Pat. 4 471 122, 1984; CA 1985; **102**: 78888.
- Baldwin JJ, Pietruszkiewicz A, Bolhofer WA, Lumma WC Jr, US Pat. 4 567 191, 1986; CA 1986; **105**: 42815.
- Stegelmeier H, Niemers E, Rosentreter U, Knorr A, Garthoff B. Ger. Pat. 3 309 655, 1984; CA 1985; **102**: 24633.
- Stone CA. Ger. Pat. 2 705 863, 1977; CA 1977; **87**: 177980.
- Stone CA. US Pat. 4 156 734, 1979; CA 1979; **91**: 211822.
- Carson J. US. Pat. 3 177 221, 1965; CA 1965; **63**: 611.
- Preiss M, Metzger KG. Ger. Pat. 2 658 906, 1978; CA 1978; **89**: 146919.
- Campbell SF, Roberts DA, Stubbs JK. Eur. Pat. 94 766, 1983; CA 1984; **100**: 121105.
- Arya VP, Nagarajan K, Shenoy SJ. *Indian J. Chem., Sect. B* 1982; **21B**: 941.
- Nagarajan K, Arya VP, George T, Nair MD, Sudarsanam V, Ray DK, Shrivastava VB. *Indian J. Chem, Sect. B.*, 1984; **23B**: 342.
- Dovlatyan VV, Mirzoyan RS. *Arm. Khim. Zh.* 1975; **28**: 412; CA 1975; **83**: 206174.
- Mirífico MV, Caram JA, Vasini EJ, Sicre JE. *J. Phys. Org. Chem.* 1993; **6**: 341.
- Caram JA, Mirífico MV, Vasini EJ. *Electrochim. Acta* 1994; **39**: 939.
- Caram JA, Mirífico MV, Aimone SL, Vasini EJ. *Can. J. Chem.* 1996; **74**: 1564.
- Wright JB. *J. Org. Chem.* 1964; **29**: 1905.
- Riddick JA, Bunger WB. In *Techniques of Chemistry*, vol. IIA, Weissberger A. (ed). Wiley-Interscience: New York, 1970; 201.

21. Perrin DD, Armarego WLF. *Purification of Laboratory Chemicals*. Pergamon Press: Oxford, 1988.
22. Coetzee JF. *Recommended Methods for Purification of Solvents and Tests for Impurities*. Pergamon Press: Oxford, 1982.
23. Person WB. *J. Am. Chem. Soc.* 1965; **87**: 167.
24. Rose NJ, Drago RS. *J. Am. Chem. Soc.* 1959; **81**: 6138.
25. Mirífico MV, Vasini EJ. *An. Quim.* 1995; **91**: 557.
26. Pretsch E, Clerc T, Seibl J, Simon W. *Tabellen zur Struktur-aufklärung Organischer Verbindungen mit Spektroskopischen Methoden*. Springer: Berlin, 1976.
27. Castellano EE, Piro OE, Caram JA, Mirífico MV, Aimone SL, Vasini EJ, Glossman MD. *J. Phys. Org. Chem.* 1998; **11**: 91.
28. Kamlet MJ, Abboud JM, Abraham MH, Taft RW. *J. Org. Chem.* 1983; **48**: 2877.
29. Svartman EL, Caram JA, Mirífico MV, Vasini EJ. *Can. J. Chem.* 1999; **77**: 511.
30. Pansare SV, Rai AN, Kate SN. *Synlett*, 1998; 623.
31. Aimone SL. Thesis. Universidad Nacional de La Plata, Facultad de Ciencias Exactas, 1999.
32. Le Hénaff P. *Bull. Soc. Chim. Fr.* 1968; 4687.
33. Knox JH. *Molecular Thermodynamics*. John Wiley & Sons: Chichester 1971; 201.